Chirped InAs/InP quantum-dash laser with enhanced broad spectrum of stimulated emission

AIP | Applied Physics Letters

Chirped InAs/InP quantum-dash laser with enhanced broad spectrum of stimulated emission

M. Z. M. Khan, T. K. Ng, Chi-Sen Lee, P. Bhattacharya, and B. S. Ooi

Citation: Applied Physics Letters **102**, 091102 (2013); doi: 10.1063/1.4794407
View online: http://dx.doi.org/10.1063/1.4794407
View Table of Contents: http://scitation.aip.org/content/aip/journal/apl/102/9?ver=pdfcov
Published by the AIP Publishing

Chirped InAs/InP quantum-dash laser with enhanced broad spectrum of stimulated emission

M. Z. M. Khan,[1] T. K. Ng,[1] Chi-Sen Lee,[2] P. Bhattacharya,[2] and B. S. Ooi[1,a)]
[1]*Photonics Laboratory, King Abdullah University of Science and Technology (KAUST), Thuwal 23955-6900, Saudi Arabia*
[2]*Department of Electrical Engineering and Computer Science, University of Michigan, 1301, Beal Avenue, Ann Arbor, Michigan 48109-2122, USA*

(Received 20 January 2013; accepted 20 February 2013; published online 4 March 2013)

We report on the demonstration of 50 nm (full-width at half-maximum) broadband stimulated emission from a chirped AlGaInAs barrier thickness multi-stack InAs/InP quantum dash (Qdash) laser. The 2 μm wide uncoated Fabry-Perot (FP) ridge-waveguide laser exhibits a total power of 0.18 W, corresponding to an average spectral power density of 3.5 mW/nm, under pulsed current conditions. Intentional extended inhomogeneity across the Qdash stacks have been attributed to the enhancement of broadband emission. © *2013 American Institute of Physics*. [http://dx.doi.org/10.1063/1.4794407]

Demonstrating broad emission spectra utilizing various active gain mediums have been the area of active research from the past decade. This includes epitaxially engineered multi-stack structures utilizing either hybrid quantum dot (Qdot)-quantum well (Qwell) or chirped Qdot (by varying capping layer thickness) and Qdash (by varying barrier thickness or InAs deposition conditions or both) nanostructures.[1–3] A wide gain bandwidth of as large as 300 nm in the O and C-L bands has been reported from these InAs/GaAs Qdot and InAs/InP Qdash structures, respectively. In device demonstration, broad amplified spontaneous emission (ASE) of ~85–150 nm have been reported from Qdot and Qdash superluminescent diodes (SLD) with emitted power in the range of a few mW.[2,4,5] The drive to overcome the trade-off between power and bandwidth in SLDs shifted the exploration to Qdot/Qdash lasers with promising results. We demonstrated a high power ~(0.6) 1.0 W broad stimulated emission ~(22) 41 nm full width at half maximum (FWHM) from as grown (intermixed) InAs/InP Qdash lasers emitting in the L (C) bands.[6–9] In the short wavelength InAs/GaAs Qdot structures, a FWHM of ~22 (75) nm with high power ~0.5 (0.75) W, has been reported, employing standard (chirped) double-heterostructure design.[10–12] This enhancement in the lasing bandwidth offered by chirping forms a potentially viable platform, and the realization of such devices would offer compact, high-efficiency, and cost-effective solution in optical communications, medical imaging, metrology, and spectroscopy and sensing.[4,5]

In this work, we investigated chirping on the multi-stack InAs/InP Qdash structure, which is accomplished by varying the AlGaInAs barrier layers. Because of the enhanced influence of vertical strain by the Qdashes on the subsequent Qdash stacking layer while maintaining reasonable electronic decoupling, we achieved an enhanced lasing bandwidth of 50 nm (FWHM) from the 2 μm wide ridge FP laser with high average spectral power density (ASPD). Our results may lead to the realization of gain and absorption regions within a single active section that forms a new structure for passive mode locked lasers. In addition, our work is an advancement of achieving ultra-wide lasing bandwidth and high power tunable devices based on monolithically integrable multi-gain section design covering C-L-U-bands.

The laser structure has 4 stacks of nominally 5 monolayers of InAs dashes, each embedded in 7.6 nm compressively strained $In_{0.64}Ga_{0.16}Al_{0.2}As$ quantum well and a varying thickness (20, 15, 10, and 10 nm) tensile-strained $In_{0.50}Ga_{0.32}Al_{0.18}As$ top barriers, and fixed 25 nm lower barrier. Remaining details of the structure could be found elsewhere.[6,7] Apart from the chirped full laser structure (CS) another similar partial structure was prepared with fixed 10 nm barrier thickness (FS). FP lasers with ridge width 2 μm and cavity length 0.36–3 mm were fabricated from the CS sample and cleaved without having reflection coatings. The processed laser bars were tested at room temperature under pulsed operation (0.5 μs pulse width and 0.2% duty cycle).

The effect of chirping the barrier thickness on the Qdashes is studied from the photoluminescence (PL) spectroscopy at 77 K under different excitations. Identical ground state (GS) emission at low (~1.54 μm at 1.5 W/cm^2) and blue shifted peak emission at high (~1.46 μm at 3 kW/cm^2) excitations, from both CS and FS samples, are apparent from Fig. 1(a). This suggests that these emission peaks are dominated by the top (S^A_{10}) and bottom (S^B_{10}) 10 nm thick barriers Qdash layers. An energy band model is shown in the inset of Fig. 1(a) for better illustration, taking into account the barrier height changes and the comparable statistical average dash heights of 2.5–3 nm (Fig. 1(b)) from the cross-sectional transmission electron microscopy (TEM), with an error margin of ±0.5 nm. The second emission hump (~1.41 μm at 3 kW/cm^2) in the CS PL spectra, shown in Fig. 1(c), which is absent in the FS spectra, indicates the GS emission originates from 15 nm (S_{15}) thick barrier Qdash layer with ~2.7 nm average dash height. It is worth mentioning that under the same high excitation density (≥300 W/cm^2), the PL FWHM of the CS sample is much wider than the FS sample. At an excitation of 3 kW/cm^2, the PL linewidth of CS (151 nm) surpasses FS (104 nm) by 47 nm. This enormously large broadening of the PL spectra is a collective contribution from different multiple transition states appearing from the extended inhomogeneous broadening

a)Electronic mail: boon.ooi@kaust.edu.sa.

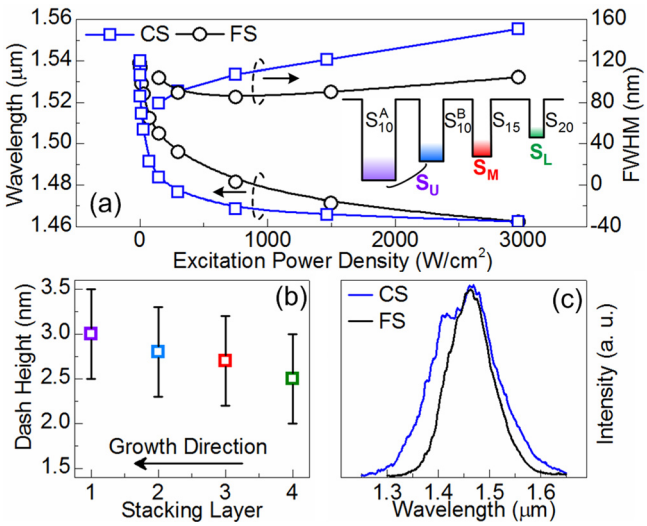

FIG. 1. (a) The peak wavelength shift and FWHM of 77 K PL at different excitation power densities. (b) Average dash height versus the stacking layers as observed from the TEM images, and (c) 77 K PL emission spectra at excitation power density of 3 kW/cm^2. The inset of (a) illustrates the conduction energy band diagram model consisting of 4 dash groups corresponding to the 4 stacks of the active region.

among the dash layers, in addition to the localized (in-plane) inhomogeneity. Deconvoluting the CS PL spectra at 3 kW/cm^2 into four Gaussian curves (fixing the peak wavelength of three curves to the above values) resulted in a peak emission wavelength ~1.37 μm from the fourth Gaussian curve which is attributed to the 20 nm (S_{20}) thick barrier Qdash layer (~2.5 nm average dash height). In general, the energy separation between these Qdash layers varies from 25 meV to 42 meV.

To further evaluate the occurrence of Qdash groups corresponding to the different stacking layers and emitting at dissimilar wavelength, in the stimulated emission regime, we tested the lasers at various cavity lengths, and the current density (J) dependent modal gain, g_{mod}, characteristics are plotted in Fig. 2(a). Fitting the data (closed symbols) with an empirical equation $g_{\mathrm{mod}} = g_{sat}(1 - \exp[-\gamma(J_{th} - J_0)/J_{th}])$ revealed emission from three distinct dash ensembles instead of four, with derived saturation modal gain g_{sat} (transparency current density J_0) of 18.5 cm^{-1} (1.82 kA/cm^2), 32.7 cm^{-1} (2.48 kA/cm^2), and 47.5 cm^{-1} (3.20 kA/cm^2). We attribute these emerging from $S_U = S_{10}^A + S_{10}^B$ (upper), $S_M = S_{15}$ (middle), and $S_L = S_{20}$ (lower) stacks, respectively. We postulate that S_{10}^A and S_{10}^B dashes contribute collectively in this regime as they correspond to identical barrier thickness, supported by various studies that show that the barrier thickness has a pronounced effect on the dash emission energy although the TEM analysis shows different average dash height among these two stacks.[13] Qualitative wavelength coverage of these dash groups are also assessed in terms of lasing wavelength (λ_{th}) obtained at 1.1 Jth (open symbols) and at different laser cavities. These are shown as shaded regions in Fig. 2(a). The emission boundaries between these groups are approximately at ~1.622 μm (±4 nm) and ~1.607 (±4 nm).

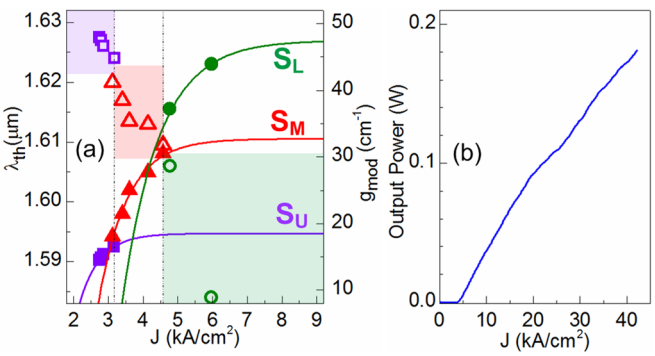

FIG. 2. (a) Qdash modal gain (closed symbols) and 1.1 Jth lasing wavelength (open symbols) versus threshold current density at room temperature, obtained from devices with different cavity lengths (0.36–3.0 mm). The lines are the theoretically fitted curves ($\gamma = 3$), and the shaded regions vaguely correspond to the emission boundaries of the three Qdash groups. The internal loss is $\alpha_i = 10.5$ cm^{-1}. (b) Room temperature L-I characteristics of 2×830 μm^2 Qdash laser.

Fig. 2(b) shows the room temperature light-current (L-I) characteristics of 0.83 mm cavity length CS Qdash laser with threshold current density of Jth = 3.6 kA/cm^2. The near threshold slope efficiency is estimated to be ~0.36 W/A, which is >2 times improvement compared to our previously reported as-grown Qdash laser.[6] The laser was able to withstand high current injection up to 11.7 Jth without showing any evidence of thermal rollover, and the measured total power at this pumping is ~0.18 W (2 facets), with a characteristics temperature T_o better than our previous reports (~60 K). Minor kink in the L-I curve between ~5 Jth and 8 Jth is observed, attributed to the energy exchange between different dash ensembles that might create unstable lasing actions from different longitudinal modes and energy levels.

The progressive room temperature lasing spectra under various pulsed current density is illustrated in Fig. 3(a). The corresponding bandwidths measured at FWHM (−3 dB), −10 dB (Δ_{-10dB}), and −25 dB (Δ_{-25dB}) levels are shown in Fig. 3(b), in addition to the ASPD (Total Power/FWHM). The spectra broaden from 1.1 Jth (2.7 nm) to 4.9 Jth (13 nm) with a single main lobe emission centered at ~1.615 μm (±1 nm). Moreover, occurrence of even larger broadening

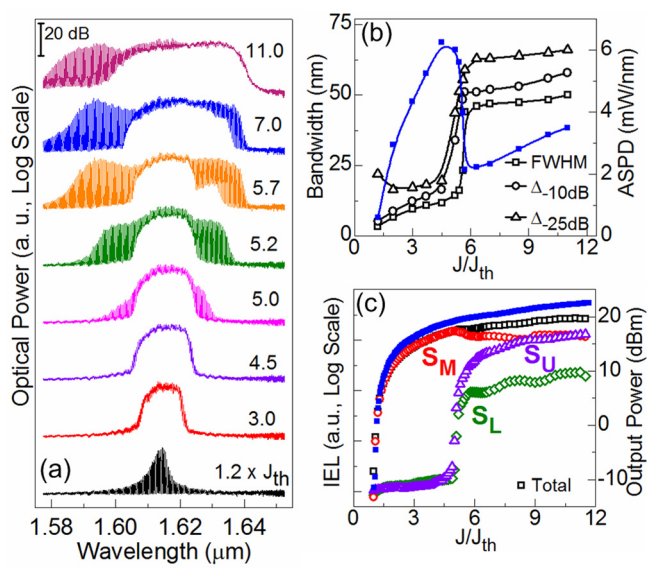

FIG. 3. (a) Room temperature lasing spectra of 2×830 μm^2 laser at increasing current injections (×Jth). (b) Bandwidth, ASPD, and (c) log IEL of the lasing spectra versus the current injection. The L-I characteristics in log scale (closed symbols) is also shown in (c). The open (closed) symbols in (b) and (c) correspond to the left (right) vertical scale.

with almost no red shift in the lasing spectra indicates negligible heating effects. The increase in the FWHM suggests collective lasing action from dashes with different geometries, attributed to S_M layer since the Δ_{-25dB} bandwidth of the main lobe is in good agreement with its wavelength coverage. At $J \approx 5$ Jth, side lobes at shorter (longer) wavelength appears on the either side of the main emission lobe implying lasing onset from the S_L (S_U) stacks. Further increase in current injection drastically enhances the lasing bandwidth, and the broadening is due mainly from the side lobe contribution. This is characterized by a sharp increase (decrease) in the slope of the FWHM (APSD) in Fig. 3(b). The appearance of kinks in the L-I curve, at those particular current injections, further corroborates our attribution. The 5.7 Jth spectrum depicts ~44 nm FWHM and $\Delta_{-10dB} \sim 51$ nm and centered at ~1.614 μm. The lasing spectrum reaches its largest bandwidth between 11 Jth and 13 Jth, with the FWHM of 50 nm and the $\Delta_{-10dB} \sim 60$ nm with ASPD ~3.5 mW/nm.

The peculiarity of this laser is the observation of three distinct emission humps in the lasing spectra, emerging from the three Qdash groups, as seen in Fig. 3(a). The progressive increase in the pumping current appreciably overlaps the GS emissions of the S_M and S_U dash ensembles, suggesting uniform distribution of dash electronic states among these highly inhomogeneous stacks. However, the distinct spectral modulation from the S_L layer persists even at higher current injection and with visible FP resonances. This implies large absorption happening in the active medium that prevents this dash group to compete evenly with other dash groups. To further assess this observation, the integrated electroluminescence (IEL) of these three dash groups are plotted separately, as a function of current injection in Fig. 3(c), following the emission boundaries discussed earlier. For injection current density <5 Jth, the lasing emission from S_M dominates, attributed to the non-ideal gain clamping in the inhomgeneously broadened gain of the other Qdashes. Increasing pump current beyond 5 Jth clearly shows initial lasing from S_U and S_L dash groups, characterized by the sharp increase in the slope of IEL curve. Note that the intensity of S_M tends to saturate at the onset of lasing of the other groups and with a constant FWHM (Fig. 3(a)). Now, the carriers are more effectively captured by the other dash groups, and the IEL indicates that S_U eventually dominates the lasing emission and competes with S_M dash groups at >7 Jth (Fig. 3(c)). This is possible in a Qdash system with dispersive geometries. Population inversion preferentially occurs in small average height S_L dashes acquiring dot-like features (tight lateral confinement, lower modal gain, and DOS) that require smaller number of carriers. The generated high-energy photons from S_L dashes get absorbed by large average height S_U dashes (weak lateral confinement, higher modal gain, and DOS). In other words, S_L dashes behave as carrier feeders in this Qdash system, demonstrated by six times less intense IEL. Nevertheless, a gradual increase in the intensities of both S_U and S_L, with increasing pumping current, suggests no saturation level observed, even at 11.7 Jth.

In conclusion, we demonstrated the emission dynamics of the chirped AlGaInAs barrier Qdash ridge-waveguide laser. A broad emission spectrum of 50 nm FWHM and ~0.18 W output power with improved slope efficiency is achieved. Our results are a step forward in achieving eventual ultra-broad emission devices covering C-L-U bands through monolithic integration of different bandgap gain sections using selective wavelength trimming methods such as quantum-dot/dash intermixing technique. Our results also indicate the feasibility to achieve absorbing and gain region within a single active medium that would be attractive in realizing mode-locking characteristics attaining the features of the two-section passive mode locking design.

The work was supported by KAUST's Competitive Research Grant (No. CRG-1-2012-OOI-010).

[1]S. Chen, K. Zhou, Z. Zhang, D. Childs, M. Hugues, A. Ramsay, and R. Hogg, Appl. Phys. Lett. **100**(4), 041118 (2012).
[2]M. Crowley, N. Patel, T. Saiz, M. El Emawy, T. Nilsen, N. Naderi, S. Mukherjee, B. Fimland, and L. Lester, Semicond. Sci. Technol. **27**(6), 065011 (2012).
[3]A. Somers, W. Kaiser, J. P. Reithmaier, A. Forchel, M. Gioaninni, and I. Montrosset, Appl. Phys. Lett. **89**, 061107 (2006).
[4]B. S. Ooi, H. S. Djie, Y. Wang, C. L. Tan, J. C. M. Hwang, X. M. Fang, J. M. Fastenau, A. W. K. Liu, G. T. Dang, and W. H. Chang, IEEE J. Sel. Top. Quantum Electron. **14**(4), 1230–1238 (2008).
[5]Z. Zhang, R. Hogg, X. Lv, and Z. Wang, Adv. Opt. Photon. **2**(2), 201–228 (2010).
[6]H. S. Djie, C. L. Tan, B. S. Ooi, J. C. M. Hwang, X. M. Fang, Y. Wu, J. M. Fastenau, W. K. Liu, G. T. Dang, and W. H. Chang, Appl. Phys. Lett. **91**, 111116 (2007).
[7]C. L. Tan, H. S. Djie, Y. Wang, C. E. Dimas, V. Hongpinyo, Y. H. Ding, and B. S. Ooi, Appl. Phys. Lett. **93**, 111101 (2008).
[8]M. Z. M. Khan, T. K. Ng, U. Schwingenschlogl, P. Bhattacharya, and B. S. Ooi, Appl. Phys. Lett. **98**, 101105 (2011).
[9]M. Z. M. Khan, T. K. Ng, U. Schwingenschlogl, P. Bhattacharya, and B. S. Ooi, Opt. Express **19**(14), 13378–13385 (2011).
[10]H. Djie, B. Ooi, X. M. Fang, Y. Wu, J. Fastenau, W. Liu, and M. Hopkinson, Opt. Lett. **32**(1), 44–46 (2007).
[11]A. Kovsh, I. Krestnikov, D. Livshits, S. Mikhrin, J. Weimert, and A. Zhukov, Opt. Lett. **32**(7), 793–795 (2007).
[12]C. S. Lee, W. Guo, D. Basu, and P. Bhattacharya, Appl. Phys. Lett. **96**(10), 101107 (2010).
[13]K. Nishi, H. Saito, S. Sugou and J. S. Lee, Appl. Phys. Lett. **74**(8), 1111–1113 (1999).